Macromolecules

Volume 41, Number 19 October 14, 2008

Communications to the Editor

Chain Entropy and Wetting Energy Control the Shape of Nanopatterned Polymer Brushes

Alain M. Jonas,*,†,§ Zhijun Hu,† Karine Glinel,‡,|| and Wilhelm T. S. Huck*,‡

Research Center in Micro- and Nanoscopic Materials and Devices (CeRMiN), Université catholique de Louvain, Place Croix du Sud 1, B1348, Louvain-la-Neuve, Belgium, and Melville Laboratory for Polymer Synthesis, Department of Chemistry, University of Cambridge, Lensfield Road, Cambridge CB2 1EW, U.K.

Received July 14, 2008
Revised Manuscript Received August 25, 2008

Surfaces displaying a nanotailored topography are frequent in nature[1] and are used for technological applications such as superhydrophobic films, optical coatings, motion control, or light-emitting devices.[1−4] The destabilization of thin layers of polymer fluids is a way to generate such surfaces of controlled topography.[5,6] However, the residual mobility of the chains affects adversely the long-term properties of the surface. This issue can be avoided by using polymer fluids with chains tethered at one end, i.e., polymer brushes.[7−9] In this respect, nanopatterned polymer brushes are optimally suited to design stable nanotailored surfaces. Such nanobrushes form nanodroplets which should wet surfaces within the constraints imposed by the tethering of the chains and by their nanometric dimensions. It is known that the seminal Young−Dupré law[10] describing the contact angle of a fluid on a surface has to be adapted when entering in the nanometer range.[11] However, how this law needs to be modified for a nanoconfined tethered fluid is still unknown, although similar complex fluids govern the functioning of natural devices like biooptical components, nuclear pore gates, or confined biopolymer networks.[1,12,13]

In this communication, we examine experimentally the shape of nanodroplets of a model polymer brush, poly(2-(2-methoxyethoxy)ethyl methacrylate), $PMEO_2MA$ (**1**, Scheme 1), and derive a general model based on chain entropy and wetting energy to describe semiquantitatively the dry shape of a nanodroplet of a polymer brush. In contrast with a previous report where the shape of nanopatterned brushes was obtained by computer simulations in a solvent,[14] the present model is developed for dry brushes and is based on a "Flory argument" involving a small set of analytical expressions directly related to the microscopic properties of polymer chains (elasticity and wetting). The model is successfully tested on the present and previously published results[15,16] and is used to explain why a universal relationship exists between the height of a nanopatterned dry brush and its lateral dimensions, when all spatial variables are scaled by the height of the corresponding brush of infinite lateral extent, h_0, as was noted before.[14,15]

Scheme 1. Chemical Structures of the Molecules Used To Fabricate Nanopatterned Brushes

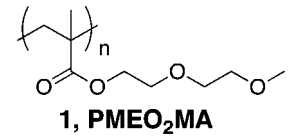

1, $PMEO_2MA$

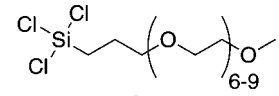

2

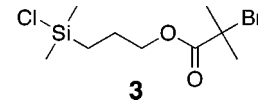

3

The growth by atom-transfer radical polymerization (ATRP) of dense brushes of $PMEO_2MA$ on silicon was reported previously,[17] as was the nanopatterning of silicon wafers by electron-beam lithography and silanation.[18] Here, we combined both methods to grow $PMEO_2MA$ brushes from silicon wafers prepatterned with an ATRP initiator (**3**, Scheme 1).

Briefly, arrays of circular holes were realized by electron beam or nanoimprint lithography in 100 nm thick poly(methyl methacrylate) (PMMA) films on silicon wafers. The wafers were

* Corresponding authors. E-mail: alain.jonas@uclouvain.be, wtsh2@cam.ac.uk.
† Université catholique de Louvain.
‡ University of Cambridge.
§ In sabbatical leave in the University of Cambridge.
|| Permanent address: PBM-UMR 6522, CNRS-Université de Rouen, France.

10.1021/ma801584k CCC: $40.75
Published on Web 09/10/2008

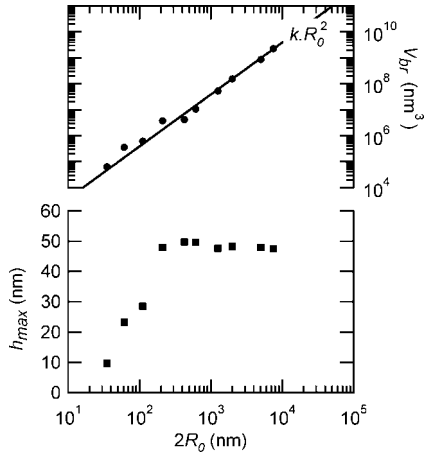

Figure 1. Maximal height h_{max} (squares, bottom) and volume V_{br} (circles, top) of a set of $PMEO_2MA$ nanobrushes grown in a single experiment versus their grafting diameter $2R_0$. The thickness of the corresponding laterally infinite brush was 48.6 nm. The background was OEO-silanized silicon. The continuous line is a R_0^2 power law, which shows volume conservation.

then reacted with the ATRP silane initiator in the gas phase, after which the PMMA mask was quantitatively removed by an acetone Soxhlet. For most samples, an oligo(ethylene oxide)silane (**2**, Scheme 1) was then deposited from solution to form a continuous background surrounding the ATRP initiator. The $PMEO_2MA$ brush was then grown from the ATRP initiator-covered regions using standard aqueous ATRP conditions.[17] The wafers were finally rinsed in methanol and water and stored in the dark in nitrogen before further use. Because each wafer supports a complete range of dot sizes, no variability arises from possible differences in polymerization conditions. A 1 μm wide line of initiator was also drawn on wafers as reference for h_0. The distance between the dots was large enough to avoid chain bridging between neighboring dots.

The nanopatterned dry brushes were observed by tapping mode atomic force microscopy (AFM) in air of constant and low relative humidity. The maximum height of the brush nanodots, h_{max}, was found to decrease with decreasing diameter of the grafting region, $2R_0$, as shown in Figure 1 (squares) for a typical set of nanobrushes grown in identical conditions over a large range of initiator dot sizes. The volume V_{br} of the nanobrushes was computed by integration of the background-subtracted AFM images (Figure 1, circles). The volume scales with the radius of the initiator dot as $V_{br} \propto R_0^2$ (continuous line in Figure 1), which indicates volume conservation since V_{br} is proportional to the area of the initiator dots. This important observation indicates that the surface-initiated polymerization process itself is not affected by the patterning, even for sizes as small as a few tens of nanometers.

Figure 2 (black squares) presents the reduced maximal height for all synthesized $PMEO_2MA$ nanobrushes, $\bar{h}_{max} = h_{max}/h_0$, versus their reduced grafting diameter, $2\bar{R}_0 = 2R_0/h_0$, determined on a series of brushes grown in different conditions, with h_0 varying from 27 to 78 nm, $2R_0$ ranging from 35 nm to 9 μm, and using two different backgrounds for the brushes, either bare silicon or oligo(ethylene oxide) (OEO)-silanized silicon. Also shown in Figure 2 are the reduced maximal heights of nanobrushes of poly(*N*-isopropylacrylamide) (PNIPAM)[15,19] and of polystyrene (PS)[16] reported by others. Considering the variety of polymers displayed in Figure 2, the large range of reference heights (27−370 nm), and the fact that the reduced diameters of the grafting regions span 3 orders of magnitude—corresponding

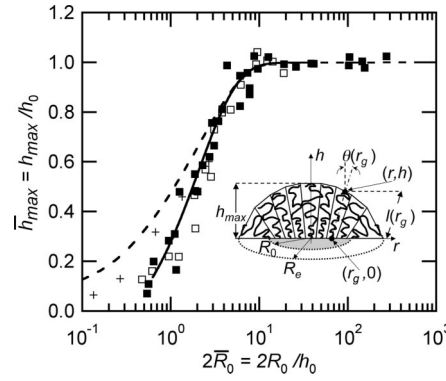

Figure 2. Reduced maximal height of nanobrushes versus their reduced grafting diameter: (■) $PMEO_2MA$ brushes; (□) PNIPAM brushes;[15] (+) PS brushes.[16] Dashed line: theoretical master curve incorporating chain entropy only. Continuous line: theoretical prediction incorporating chain entropy and wetting energy (with $h_0 = 50$ nm). The inset is a scheme of a brush nanodroplet.

to real diameters ranging from 35 nm to a few μm—the collapse of all data points on a single master curve is remarkable.

The reasons for the existence of a master curve, and the master curve itself, can be derived by geometry and macromolecular physics. Consider a chain grafted on a dot of initiator as shown in Figure 2 (inset); its footprint on the surface is σ, and it tilts away from the normal to the surface by an angle θ because of the lateral spreading of the chains at the edge of the brush. The chain is assigned a volume V, which is the volume occupied by its segments. Assuming incompressibility, which is a good approximation for a rubbery material, each volume V is equal to a single reference volume $V_0 = h_0\sigma$. Because the chains grafted far away from the center of the dot are more tilted than the chains grafted near the center, the length of this volume, l, is smaller for chains at the periphery than farther in the interior of the dot. V can be computed by volume integration; in the continuous limit when the grafting density is large, one finds (see Supporting Information for details)

$$V(r_g) \approx h_0\sigma\left[\bar{l}^3\frac{\dot{\theta}_{\bar{r}}\sin\theta}{3\bar{r}_g} + \bar{l}^2\left(\frac{\sin 2\theta}{4\bar{r}_g} + \frac{1}{2}\dot{\theta}_{\bar{r}}\right) + \bar{l}\cos\theta\right] = h_0\sigma \quad (1)$$

where r_g is the radius at which the chain is grafted, $\bar{l} \equiv l/h_0$, $\bar{r}_g \equiv r_g/h_0$, and $\dot{\theta}_{\bar{r}} = \partial\theta/\partial\bar{r}_g$. This equation shows that the reduced length of the volume associated with a chain, $\bar{l}$, depends only on the tilt angle of this volume, θ, and on the reduced radius at which the chain is grafted, $\bar{r}_g$. Importantly, this relationship does not involve polymer-dependent parameters, since σ and h_0 factor out on both sides of eq 1. In other words, the geometrical relationship between the reduced length and the reduced radius of grafting is unique.

The entropy of a stretched chain is proportional to the square of its end-to-end distance.[20,21] Previous modeling of laterally infinite brushes, such as by the strong stretching theory[22] or the complete self-consistent field theory,[23] has shown that free chain ends are distributed along the vertical distance in a dry brush and are not localized at its outer surface. Nevertheless, we assume in the sequel that the entropy of a chain is simply related to the square of l, thereby effectively neglecting the distribution of the positions of the chain ends in the brush. This approximation corresponds to a "Flory argument" as proposed initially by Alexander[7] and de Gennes[8] for laterally infinite brushes; it is known to represent properly, within some factors of order unity,[9]

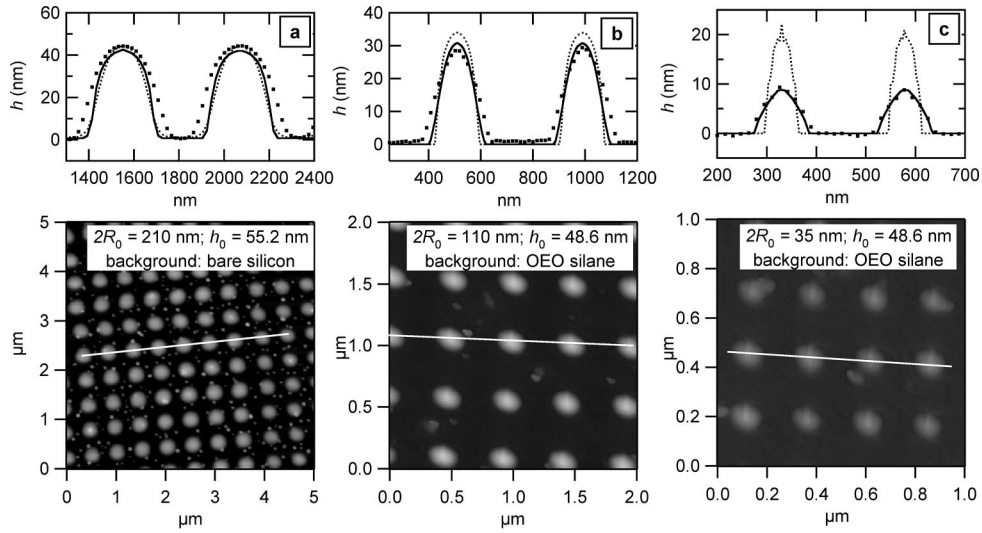

Figure 3. AFM topographic images of $PMEO_2MA$ dry nanobrushes and height profiles along part of the white lines drawn in the images (■). The dotted line is the prediction from a model incorporating chain entropy only; the full line is from the complete model incorporating chain entropy and wetting energy. Note that partial broadening of the experimental profiles arises due to image dilation by the shape of the AFM tip.

properties such as brush height, free energy per chain, and stretching−repulsion balance, which are precisely the properties we are interested in. In addition, the small polydispersity of the chains is neglected in the sequel, since the brushes were grown by controlled radical polymerization for short times only (less than 2 h). The entropy of the confined brush then reads $S_{br} = (-3k/2Nb^2)\sum l^2$, where b is the Kuhn length of $PMEO_2MA$, N is the number of Kuhn segments, and the sum extends over all chains in the nanobrush. In the continuous limit

$$S_{br} = -\frac{3k}{2Nb^2}\frac{1}{\pi {R_0}^2}\int_0^{R_0} l^2(r_g)2\pi r_g \, dr_g \propto \int_0^{\bar{R}_0} \bar{l}^2(\bar{r}_g)\bar{r}_g \, d\bar{r}_g \quad (2)$$

The shape of the nanobrush, $h(r)$, was obtained numerically by finding the function $\theta(r_g)$ allowing to maximize entropy (eq 2), under the constraint set by eq 1 and while setting $\theta(0) = 0$, $\theta(r_g = R_0) = \pi/2$, and $\partial\theta/\partial r_g \geq 0 \ \forall r_g \in [0, R_0]$. The first condition is required by symmetry, the second derives from the fact that the chains lie on the substrate at the periphery of the dot, and the third assumes a regular fanning out of the chains from the center toward the outskirts of the nanodot. The height profile of the nanobrush is $(r, h) = (r_g + l\sin(\theta), l\cos(\theta))$ (Figure 2, inset), from which the reduced maximal height $\bar{h}_{max}$ is obtained.

The so-obtained theoretical relationship between $\bar{h}_{max}$ and $2\bar{R}_0$ is shown in Figure 2 (dashed line); it is a master curve of purely geometric and entropic nature, with no parameter specific to the polymer considered since polymer-dependent parameters appear only as prefactors in an expression to be maximized (eq 2). This explains why the experimental points obtained for different polymers almost fall on a single curve. The agreement between the entropy-based theoretical master curve and the experimental data is reasonably good, with the first part of the decrease of $\bar{h}_{max}$ being well-reproduced by the theoretical prediction. The decrease of the maximal height to a value below the one of the laterally infinite brush starts for reduced dot diameters below 10, as observed experimentally. This value of $2\bar{R}_0$ may be taken as the value from which confinement effects begin to affect the whole nanobrush, as opposed to being limited to the edges of the brush only. This corresponds to diameters as large as half a μm for a brush of 50 nm reference height only; for a much thicker brush of 500 nm, confinement effects would already appear for dot diameters as large as 5 μm.

For $2\bar{R}_0 \leq 3$, the agreement between prediction and experiments is lost, as can also be checked on the height profiles of selected nanobrushes shown in Figure 3 (dotted lines). Figure 3a is the experimental height profile of brushes of 3.8 reduced grafting diameter, together with the theoretical model. The agreement between model and experiment is excellent, considering that a slight broadening of the nanobrush profile arises from the AFM imaging process. When $2\bar{R}_0$ is decreased to a value of about 2.3 (Figure 3b), the model overestimates the height of the nanobrush by about 20%. When it is decreased further to ~0.7 (Figure 3c), the model fails completely, with the height of the nanobrush being overestimated by 130%, whereas its width is clearly underestimated.

The reason for the failure of the entropy-based model for the more strongly confined nanobrushes stems from our neglect of the (partial) wetting of the substrate by the chains of the nanobrush. The nanobrush is also a nanodroplet of a substrate-anchored fluid and thus has to respect boundary conditions at the contact line with the substrate. Because the surface-to-volume ratio of nanobrushes increases when R_0 decreases, surface energy enters the problem for small R_0. It is possible to take wetting into account by minimizing the Helmoltz free energy of the nanobrush, $F_{br} = E_{br} - TS_{br}$, instead of maximizing its entropy alone. However, this implies that energy terms specific to the polymer and the substrate be introduced in the problem, thereby decreasing the generality of the equations.

The excess surface energy of the brush with respect to the bare substrate, E_{br}, depends on the shape of the nanobrush according to

$$E_{br} = \gamma A + (\gamma_{bs} - \gamma_s)\pi({R_e}^2 - {R_0}^2) + (\gamma_{bi} - \gamma_i)\pi {R_0}^2 + \int_0^{R_e} \frac{-H}{12\pi h^2} 2\pi r \, dr \quad (3)$$

The first term of eq 3 is the energy of the surface of the nanobrush exposed to air; it involves the surface tension of the brush in air, γ, and its area exposed to air, A. The second term is the excess surface energy of the annular portion of the brush in contact with the background substrate at the rim of the dot; it depends on the interfacial tension between the brush and the background, γ_{bs}, on the surface tension of the background, γ_s, on the contact radius of the brush with the substrate, R_e, and on R_0 (Figure 2, inset). The third term is the excess surface energy of the portion of the brush lying just above the dot of initiator. This term is irrelevant because it is a constant independent of the detailed shape of the nanobrush since the polymer chains

are always in full contact with the initiator dot. The final term is an approximation for the van der Waals energy of the nanobrush sandwiched between air and Si, where H is the Hamaker constant of this system.[24] It was shown before that concepts developed for mesoscopic scales, such as contact angle and surface tension, are still valid at the nano scale.[25] However, corrections to the Young−Dupré law have to be considered, either by introducing a line tension parameter or by directly considering the presence of an effective interface potential,[11,26] which is the reason for the introduction of this fourth term.

The free energy was minimized numerically, using the material parameters given in the Supporting Information, which were taken or adapted from the literature.[27−31] The grafted area per chain σ was set to 3 nm^2, considering that values of 1.53−1.7 nm^2 were determined for brushes of PMMA grown by ATRP on silicon[32,33] and that the molar mass of MEO_2MA is about twice the one of methyl methacrylate. The predicted $\bar{h}_{max}$ is plotted versus $2\bar{R}_0$ in Figure 2 (continuous line). The agreement between model and experiment is now excellent over the whole range of dimensions. Selected predicted brush profiles are displayed in Figure 3 (continuous lines), showing that the complete model represents well the shape of $PMEO_2MA$ nanobrushes down to 35 nm grafting diameter. Given the approximation used for the location of free chain ends, the quantitative agreement between prediction and experiment may seem coincidental. However, one should be aware that the model essentially describes the deviation of the height of the nanodroplets compared to the one of the laterally infinite brush. The final droplet shape is obtained by multiplication of the reduced height by h_0, which is taken from experiments. If we assume that the vertical distribution of free chain ends is not strongly different in nanopatterned and laterally infinite brushes, a simple "Flory argument" should thus be sufficient to describe the perturbation resulting from the nanopatterning, as is observed here.

This agreement also confirms that the shape of nanobrushes is controlled by both chain entropy and wetting. If the nanobrush was a nanodroplet of a simple fluid, its contact angle with the substrate would be determined by the Young−Dupré equation[10] (or a modification of this equation including van der Waals forces for the smaller droplets).[11] In the case of an OEO−silane background for which $\gamma \approx \gamma_s$ and $\gamma_{bs} \approx 0$ (Supporting Information), the Young−Dupré equation predicts complete wetting with a contact angle of 0°. However, because of their tethering to the surface, the $PMEO_2MA$ chains resist spreading on the background, since this would result in a large decrease of entropy. The actual contact angle measured on the curves of Figure 3 is 17°−21°, quite larger than predicted by the Young−Dupré equation for the untethered polymer. This illustrates the importance of the entropic component in the determination of the shape of nanobrushes. Nevertheless, because the chains at the rim of the nanobrushes tend to spread more on the surface compared to the situation where wetting is ignored, extra room is left available for chains farther toward the center, which results in a decreased height of the nanobrush when compared to the case where entropy only is considered. This effect is lost for larger diameters because the conditions of contact at the edges are not felt far away into the dot; the average height of the nanobrush becomes thus identical irrespective of whether wetting effects are included or not.

Finally, it is also interesting to examine the relative contributions of surface energetic and van der Waals components in eq 3. The van der Waals contribution to the energy of a brush (h_0 =48.6 nm) is 7.4%, 3.4%, and 1.3% for brushes of grafting diameter $2R_0$ = 35, 60, and 110 nm, respectively. For larger R_0's, the van der Waals contribution becomes negligible. For brushes of larger h_0, the contribution of the van der Waals component will be even lower. Therefore, the shape of the nanobrushes can essentially be predicted from chain entropy and surface tensions, neglecting the van der Waals contribution. In Figure 2, the data points of PNIPAM and $PMEO_2MA$ are superimposed. This is consistent with the observation that both PNIPAM and $PMEO_2MA$ are polar and H-bonding polymers which display a similar behavior in water, with LCST's at about 30 °C.[17] It is thus reasonable to assume that they exhibit similar surface and interfacial tensions as well. Polystyrene, however, is an apolar polymer having significantly different interfacial and surface tensions; this explains why the curve related to PS does not superimpose on the ones of PNIPAM and $PMEO_2MA$ in Figure 2, in the range of dimensions where the wetting energy becomes important relative to entropy.

In conclusion, polymer nanobrushes were prepared for grafting diameters down to 35 nm. The shape of the nanobrushes in the dry state was well-reproduced by a model based on a "Flory argument", involving the entropy penalty associated with chain stretching and the energetic advantage to spread chains on a wetted substrate. When the wetting energy is ignored, a fully general master curve can be derived relating brush height and grafting diameter, once normalized by the height of the corresponding laterally infinite brush. This entropy-based master curve fails to represent properly the nanobrushes for reduced diameters below ~3. Below this value, the surface and interfacial energy contributions become important, and the nanobrushes have to be considered as nanodroplets whose shapes are controlled by wetting and chain stretching, and which depend on the specific polymer and substrate considered. Importantly, the results described here also indicate that the surface-initiated polymerization itself is not significantly influenced by the surface pattern. This is testified by the conservation of the volume of the nanobrushes and by the good agreement between model and experimental data. The method we used to derive the shape of the nanobrush could be easily generalized to other geometries or even to systems displaying a spatially varying grafting density. It is thus now possible to design rationally polymer brush surfaces displaying a complex nanotopography, without having to proceed by a time-consuming trial-and-error experimental method.

Acknowledgment. Financial support was provided by the French Community of Belgium (ARC 06/11-339), the Belgian Federal Science Policy (IAP/V/27), and the Leverhulme Trust (UK). Scientific support by B. Nysten (AFM) is gratefully acknowledged.

Supporting Information Available: Derivation of eq 1 and of expressions appearing in eq 3; material parameters (surface and interfacial tensions, Hamaker constant, geometric dimensions of the chains) used to compute the free energy; and numerical procedure used to maximize entropy or minimize free energy. This material is available free of charge via the Internet at http://pubs.acs.org.

References and Notes

(1) Lee, L. P.; Szema, R. *Science* **2005**, *310*, 1148–1150.
(2) Li, X.-M.; Reinhoudt, D.; Crego-Calama, M. *Chem. Soc. Rev.* **2007**, *36*, 1350–1368.
(3) Santer, S.; Kopyshev, A.; Donges, J.; Yang, H.-K.; Ruhe, J. *Adv. Mater.* **2006**, *18*, 2359–2362.
(4) Lee, Y.-J.; Kim, S.-H.; Huh, J.; Kim, G.-H.; Lee, Y. H.; Cho, S.-H.; Kim, Y.-C.; Do, Y. R. *Appl. Phys. Lett.* **2003**, *82*, 3779–3781.

(5) Higgins, A. M.; Jones, R. A. L. *Nature (London)* **2000**, *404*, 476–478.
(6) Leopoldes, J.; Damman, P. *Nat. Mater.* **2006**, *5*, 957–961.
(7) Alexander, S. *J. Phys. (Paris)* **1977**, *38*, 983–987.
(8) de Gennes, P.-G. *Macromolecules* **1980**, *13*, 1069–1075.
(9) Milner, S. T. *Science* **1991**, *251*, 905–914.
(10) de Gennes, P.-G.; Brochard-Wyart, F.; Quéré, D. *Capillarity, Wetting Phenomena*; Springer: New York, 2004.
(11) Yeh, E. K.; Newman, J.; Radke, C. *Colloids Surf., A* **1999**, *156*, 137–144.
(12) Lim, R. Y.; Fahrenkrog, B.; Koeser, J.; Schwarz-Herion, K.; Deng, J.; Aebi, U. *Science* **2007**, *318*, 640–643.
(13) Claessens, M. M. A. E.; Tharmann, R.; Kroy, K.; Bausch, A. R. *Nat. Phys.* **2006**, *2*, 186–189.
(14) Patra, M.; Linse, P. *Nano Lett.* **2006**, *6*, 133–137.
(15) Lee, W.-K.; Patra, M.; Linse, P.; Zauscher, S. *Small* **2007**, *3*, 63–66.
(16) Steenackers, M.; Kueller, A.; Ballav, N.; Zharnikov, M.; Grunze, M.; Jordan, R. *Small* **2007**, *3*, 1764–1773.
(17) Jonas, A. M.; Glinel, K.; Oren, R.; Nysten, B.; Huck, W. T. S. *Macromolecules* **2007**, *40*, 4403–4405.
(18) Pallandre, A.; Glinel, K.; Jonas, A. M.; Nysten, B. *Nano Lett.* **2004**, *4*, 365–371.
(19) Because the authors of ref 15 grafted brushes from small gold posts of 40 nm height protruding over the background, we only report their data when $h_{max} \gg 40$ nm, conditions for which the disturbance of chain packing by the finite height of the gold post can be neglected.
(20) Gedde, U. W. *Polymer Physics*; Chapman and Hall: London, 1995.
(21) Rubinstein, M.; Colby, R. H. *Polymer Physics*; Oxford University Press: Oxford, 2003.
(22) Milner, S. T.; Witten, T. A.; Cates, M. E. *Macromolecules* **1988**, *21*, 2610–2619.
(23) Matsen, M. W. *J. Chem. Phys.* **2004**, *121*, 1938–1948.
(24) Parsegian, V. A. *Van der Waals Forces—A Handbook for Biologists, Chemists, Engineers, Physicists*; Cambridge University Press: Cambridge, 2006.
(25) Milchev, A. In *Computer Simulations in Condensed Matter Systems: From Materials to Chemical Biology*; Ferrario, M., Ciccotti, G., Binder, K., Eds.; Springer: Berlin, 2006; Vol. *2*, pp 105−126.
(26) Checco, A.; Guenoun, P.; Daillant, J. *Phys. Rev. Lett.* **2003**, *91*, 186101/1–4.
(27) Baralia, G. G.; Filiatre, C.; Nysten, B.; Jonas, A. M. *Adv. Mater.* **2007**, *24*, 4453–4459.
(28) van Oss, C. J.; Chaudhury, M. K.; Good, R. J. *Chem. Rev.* **1988**, *88*, 927–941.
(29) Visser, J. *Adv. Colloid Interface Sci.* **1972**, *3*, 331–363.
(30) Kerle, T.; Yerushalmi-Rozen, R.; Klein, J.; Fetters, L. J. *Europhys. Lett.* **1998**, *44*, 484–490.
(31) Brandrup, J.; Immergut; E. H. *Polymer Handbook*, 3rd ed.; J. Wiley and Sons: New York, 1989.
(32) Jones, D. M.; Brown, A. A.; Huck, W. T. S. *Langmuir* **2002**, *18*, 1265–1269.
(33) Ohno, K.; Morinaga, T.; Koh, K.; Tsujii, Y.; Fukuda, T. *Macromolecules* **2005**, *38*, 2137–2142.

MA801584K